ACS EARTH AND SPACE CHEMISTRY

http://pubs.acs.org/journal/aesccq

Article

Abiotic Emission of Volatile Organic Compounds from the Ocean Surface: Relationship to Seawater Composition

Stephanie R. Schneider,* Douglas B. Collins, Matthew Boyer, Rachel Y.-W. Chang, Michel Gosselin, Victoria E. Irish, Lisa A. Miller, and Jonathan P. D. Abbatt

Cite This: *ACS Earth Space Chem.* 2024, 8, 1913−1923

Read Online

ACCESS | Metrics & More | Article Recommendations | Supporting Information

ABSTRACT: An important goal in marine atmospheric chemistry is to determine the impact of the surface ocean on the overlying marine boundary layer in terms of the ocean's potential to release volatile organic compounds (VOCs) that may impact atmospheric oxidizing capacity and aerosol growth. In addition to direct biogenic production of VOCs that are eventually emitted to the atmosphere, abiotic mechanisms that produce VOCs include direct or sensitized photochemistry and oxidation reactions initiated by gas phase oxidants. In this laboratory study, we use proton-transfer-reaction mass spectrometry to measure the emission fluxes resulting from both UV irradiation and ozone oxidation of Arctic surface microlayer water and the underlying bulk seawater. Under our experimental conditions, both mechanisms lead to comparable VOC emission fluxes, which scale closely with the total and dissolved organic carbon content of the sample. However, the composition of the seawater sample can strongly affect the emission fluxes of specific molecules. For example, nonanal fluxes from oxidation correlate closely with the phytoplankton abundance in the samples, indicating that unsaturated lipids may be the substrate. Conversely, the best predictor for the nitrogenated VOC flux under irradiation conditions is photosynthetic prokaryotes (i.e., cyanobacteria) abundance. Similar studies in a wider range of environments, ideally conducted in the field, will better constrain the importance of these abiotic processes to global ocean-to-atmosphere fluxes.

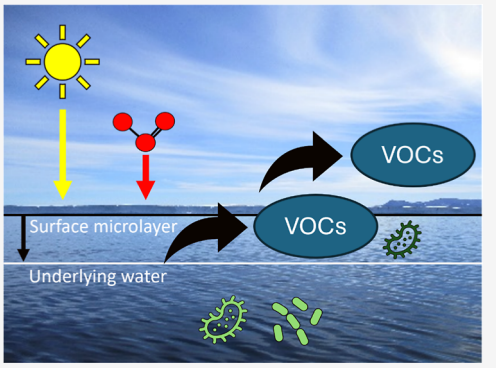

KEYWORDS: *volatile organic compounds, photochemistry, multiphase oxidation, Arctic ocean, proton-transfer-reaction mass spectrometry, sea-surface microlayer*

INTRODUCTION

The surface ocean is an important interface to the atmosphere, representing 70% of Earth's surface. The first few microns of the ocean surface in direct contact with the atmosphere are defined by a chemically distinct layer called the surface microlayer (SML). The composition of the SML can differ relative to underlying water when semisoluble or insoluble compounds move to the surface via physical processes like mixing, diffusion, or scavenging by bubbles.[1,2] Additionally, atmospheric deposition can alter the SML composition relative to underlying water.[1,3−5] The unique composition of the SML can change biological activity relative to the underlying water, which can further drive changes to the chemical composition.[6,7] The depth of the SML is operationally defined by the method used to sample it and typically ranges from 1 to 1000 μm.[1,8,9]

The surface ocean is a recognized source of volatile organic compounds (VOCs) to the marine atmosphere, but the role of the SML is still largely unclear. VOCs arising from biotic and abiotic sources in the SML can impact climate and air quality, since the VOCs can potentially be oxidized to contribute to secondary organic aerosol mass[10−12] and affect the oxidative budget of the marine atmosphere.[13−17] The SML can also physically affect the emission of VOCs into the atmosphere by damping turbulence.[18−20]

While there is no doubt that abiotic mechanisms contribute to the emission of VOCs from the SML, open questions remain about their speciation and yield, with past studies having mostly focused on the production of VOCs from photochemical mechanisms.[21] Early work found the production of low molecular weight carbonyls was enhanced in collected SML samples compared to subsurface waters.[13] Formation rates of low molecular weight carbonyls were correlated with increasing chromophoric dissolved organic matter (CDOM) in the SML, and thus photosensitizers are thought to be important.[16,22,23] Conversely, laboratory studies show that marine-derived dissolved organic matter (DOM) is a

Received: June 7, 2024
Revised: July 29, 2024
Accepted: August 9, 2024
Published: August 26, 2024

less efficient photosensitizer than terrestrial and single-component photosensitizers, highlighting the need for marine-relevant photosensitizers during laboratory experiments.[24] Experiments using the surfactant nonanoic acid, a common single-component SML proxy, found that it could act as its own photosensitizer.[22] Recent progress suggests that contaminants in commercial nonanoic acid are responsible for instigating the photosensitized chemistry, but the results nevertheless support the idea that photosensitized chemistry can be a source of VOCs at the ocean interface.[25] These studies highlight the potential role of the SML on the production of VOCs. However, there are only a few studies that have characterized a wide range of VOCs emitted from the irradiation of authentic SML samples.

Compared to photochemical studies, there have been fewer studies investigating the production of VOCs via heterogeneous oxidation with ozone of SML samples collected from the environment.[17,26,27] The VOCs formed from the heterogeneous ozonolysis of the SML collected from both the eastern equatorial Pacific ocean and the west coast of Canada were similar to those formed from the oxidation of a linoleic acid SML proxy, suggesting that unsaturated fatty acids in the SML are the major reactive component.[17] Riverine SML samples collected in the Pearl River (China) emitted nitrogenated VOCs when oxidized heterogeneously with ozone, indicating other, unknown organic precursors distinct from fatty acids.[28] Ozone also reacts quickly with dissolved iodide, which is thought to be the primary driver for ozone marine dry deposition.[29−32] The reacto-diffusive depth of ozone with respect to environmentally relevant concentrations of iodide is only a few microns, and thus the organic composition of the first few microns of the ocean is vital in determining VOC speciation and yield.[33] In the case of iodide, concentrations near the interface are reduced upon reaction with ozone without sufficient upward mixing.[33] It remains unclear how VOC production from heterogeneous ozonolysis of collected SML samples depends on waterside replenishment pathways.

Understanding abiotic emissions requires an understanding of the chemically complex and dynamic environment of the SML. Previous studies have typically represented the SML with a single model compound, such as 1-octanol, linoleic acid, or nonanoic acid.[17,22,34] Use of single component SML proxies has led to an improved understanding of the underlying chemical mechanisms which form VOCs, but such studies do not accurately represent the biological processes that play a role in determining the composition of the Arctic SML.[1,14,20] Mesocosm studies can capture the biological complexity of the Arctic SML, but it is still challenging to disentangle abiotic sources of VOCs from biotic sources.[35] Other studies have used biological cultures (e.g., phytoplankton or biofilms) to create reproducible, biologically relevant, and chemically complex SML proxies.[12,36] These proxies can bridge the gap between single component SML proxies and real seawater experiments. Work using biological systems to represent the SML show that biological life stage impact VOC yield from both heterogeneous ozonolysis and photosensitized chemistry, indicating a dependence on specific reactive precursors.[12,36] Ultimately, studying the role of the SML on VOC emission requires an interdisciplinary approach that combines ocean science, atmospheric science, biology, and chemistry.

The overarching goal of this study is to investigate the properties of seawater that affect the formation of VOCs from photosensitized chemistry and heterogeneous ozonolysis (hereafter referred to as "oxidation" in the context of these experiments) from seawater collected in the Canadian Arctic. The VOCs produced from paired bulk Arctic seawater and Arctic SML samples are compared to examine the specific role played by the Arctic SML. To our knowledge, this is the first study where the emissions from the two abiotic VOC production mechanisms are compared using the same seawater. To help with our mechanistic understanding, we compare the results from the natural Arctic samples to those from an Arctic SML proxy generated by the centric marine diatom *Thalassiosira pseudonana*.

METHODS & MATERIALS

T. pseudonana Cultures and Synthetic Seawater. *T. pseudonana* (CCMP1335) were grown in axenic conditions, as described previously.[12] Briefly, the cultures were grown in 75 mL of L1 growth media with a 12 h light/dark cycle. Aliquots of the *T. pseudonana* cultures were tested for bacterial contamination using the *f*/2 Freshwater Medium and Test Medium provided by the Bigelow National Center and compared to a positive control. Cultures were used between 20 and 24 days of growth.

The synthetic seawater solution consisted of 0.55 M of NaCl (>99.0%, Sigma-Aldrich) and 0.84 mM of KBr (>99%, Sigma-Aldrich), which was mixed with a 0.1 M phosphate buffer (sodium phosphate monobasic, ≥99.0%, Sigma-Aldrich & sodium phosphate dibasic, ≥99.0%, Sigma-Aldrich) solution to give a final pH of 8.0 ± 0.1.

For experiments, 30 mL of the *T. pseudonana* cultures (or L1 growth media) were mixed with the synthetic inorganic seawater solution, to reach environmentally relevant concentrations of organic matter.[37] KI (>99.99%, Sigma-Aldrich) was added to the final solution of *T. pseudonana* and synthetic seawater to give a final iodide concentration of 390 nM.

Arctic Sample Collection & Auxiliary Analysis of Arctic Samples. Arctic surface water was collected using a surface skimmer catamaran deployed from the CCGS Amundsen in July and August as part of the 2016 NETCARE cruise in Smith Sound (station 9), the North Water (station 7) and Southern Baffin Bay (station 2) in the Canadian Arctic (Figure S1). Bulk water samples from 0.2 m were collected through Teflon tubing deployed beneath the skimmer while SML samples were collected on surface-mounted rotating glass plates, which were manually turned between 11 and 18 rotations per minute, over a period of about 20 min, for an average collected SML volume of 3 L and thickness of 80 μm. Samples were transferred from HDPE Nalgene bottles mounted on the skimmer into glass bottles and were kept frozen (−20 °C) until the irradiation and oxidation experiments were conducted in June (sample 9) and November (sample 2 and 7) 2022. For the VOC production experiments, the samples were removed from the freezer and thawed in a 4 °C refrigerator for 24 h, then divided into two aliquots (i.e., one-half of the volume for oxidation and one-half for irradiation). More details about the sampling procedures and conditions are provided elsewhere.[38] A summary of the samples is presented in Table S1. Measurement details for total organic carbon (TOC), dissolved organic carbon (DOC), total nitrogen (TN), total dissolved nitrogen (TDN), chlorophyll *a* (an index of phytoplankton biomass), phytoplankton abundance (including photosynthetic prokaryotes and eukaryotes), heterotrophic bacterial abundance, and

https://doi.org/10.1021/acsearthspacechem.4c00163
ACS Earth Space Chem. 2024, 8, 1913−1923

surfactants are detailed in the Supporting Information in Section 1.

Experimental Configuration. The oxidation experiments were performed in a similar setup to one used previously (Figure 1A).[33,37] Briefly, the water samples sit in a quartz

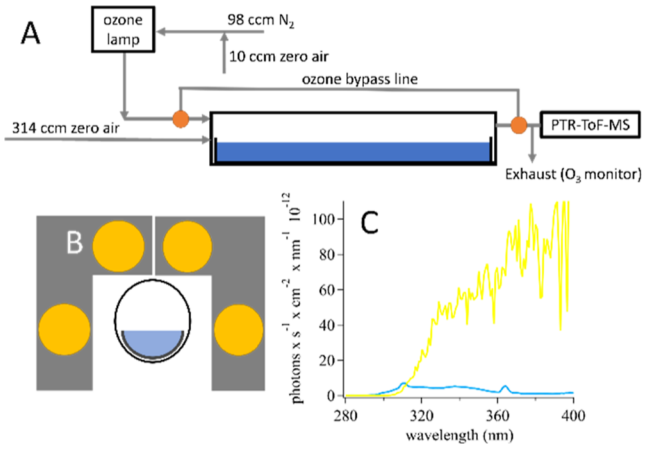

Figure 1. Summary of the experimental setup for both the ozone oxidation and the irradiation experiments. Panel A illustrates the flow system, which was used for both experiments. For the irradiation experiments, the ozone generation lamp was off, and the flow was consistently flowing through the tube, even for background measurements. Panel B shows an end-on view of the modifications for the irradiation experiments, with the addition of four UVB lamps (orange circles) around the flow tube. Panel C compares the measured spectra in the flow tube (blue) to the modeled Arctic solar flux (yellow) to represent the Arctic summer when measurements were made.

"boat" within a glass flow reactor through which gases flow at atmospheric pressure with an average residence time of 1.4 min. The largest difference from past experiments was that the ozone in this experiment was maintained at a mixing ratio of 45 ± 2 ppb, as measured with a UV photometric ozone analyzer (Thermo model 49i). The ozone mixing ratio was measured for 15 min at the beginning of each experimental day from the exhaust line with a small additional flow of clean air to meet the flow requirements of the UV ozone analyzer.

The system was adapted for the irradiation experiments with four 15 W UVB T8 fluorescent lights (Zilla 13991) added to surround the flow tube (Figure 1B). Figure 1C shows the photon flux in the experimental setup, compared to the station 2 location (Figure S1) as calculated with the TUV calculator for July 28th, 2016 at 12:00, for a latitude of 67.2869 and longitude of −63.3696 with no cloud cover (https://www.acom.ucar.edu/Models/TUV/Interactive_TUV/, last accessed May 2023). We note that the air temperature inside the tube did not increase more than 1 °C over a 90 min irradiation experiment.

For each experiment, 200 mL of sample (either a *T. pseudonana* extract in artificial seawater or an Arctic water sample) was introduced into the flow tube and left to equilibrate 1 h before starting the oxidation or illumination process. The samples were oxidized or irradiated for a minimum of 25 min, and a maximum of 90 min. After the lights were turned off, or the ozone was switched to bypass the flow tube, the decay of the VOC signal was monitored for 15 min. To validate this experimental approach, we reproduced experiments on nonanoic acid from the literature (Figure S2), as discussed in Section 2 of the Supporting Information. Background measurements were made in triplicate on the empty flow tube (for Arctic samples) or the L1 growth media (for *T. pseudonana* experiments).

VOC Measurements. The VOCs were measured using a proton transfer reaction time-of-flight mass spectrometer (PTR-ToF-MS, ToFWerk, hereby referred to as "PTR-MS"), which has a mass resolution of about 8000 at m/z 200. A sample flow into the PTR-MS of 100 cubic centimeters per minute (ccm) was maintained throughout the experiment. Average spectra were acquired from the instrument every 6 s between m/z 40 to 500 and analyzed using Tofware v3.2.3. Peaks were given molecular formulas based on the peak assignment function in Tofware (using C, H, N, O, S, I, Cl and Br atoms), looking for both protonated molecular ions ($[M + H]^+$) or water clusters of protonated molecules ($[M + H_3O]^+$). Molecular assignments were evaluated using existing molecular formula conventions and known fragments present in the PTR library.[39,40] If no reasonable molecular formula was generated using the peak assignment function, the mass spectral feature was left unassigned and referred to by its observed mass-to-charge ratio. The VOCs emitted from the natural Arctic bulk seawater and SML samples were identified using a nontargeted approach (Figure S3A). Importantly, to ensure an identical comparison, all the ions identified across all samples (both natural and cultured) were included in the high-resolution fitting of the mass spectra of each sample, even if certain ions were not initially captured by the nontargeted analysis filters in an individual experiment.

The PTR-MS was calibrated with a mixture of VOCs, including acetaldehyde, acrylonitrile, acetone, isoprene, 2-butanone and α-pinene using a standard gas cylinder (Apel-Reimer Inc.). To correct for different sensitivities of the instrument on different days, the average sensitivity of a subset of calibrant ions was taken within 2 days of each individual experiment (listed in Table S2) and applied to all the ions for the total VOC measurements, and any ions which were not directly calibrated. For the specific study of acetone and acetaldehyde below, the sensitivities of the corresponding ions were used instead of the average sensitivity.

Data Analysis. An illustrated description of the analysis workflow is described in Figure S3, which summarizes the generation of the data and plots presented in this manuscript. The signal present for the first 10 min at the start of each experiment, before exposure to light or ozone, was corrected to zero by fitting the time period before irradiation/oxidation for each individual ion to a linear function, whose extrapolation was subtracted from the entire experimental data set (Figure S3B). The remaining increase in signal is then attributed to exposure to light/ozone alone. In rare cases with poor fits, an exponential decay function was applied instead. This process was repeated for all experiments and for the background controls of an empty flow tube (for Arctic samples) or the L1 growth media (for *T. pseudonana* experiments).

The increase in signal measured between 10 and 25 min of irradiation/oxidation during the background experiments (i.e., an empty tube or L1 growth media) was subtracted from the increase in signal measured between 10 and 25 min after the irradiation/oxidation of the sample (i.e., natural Arctic samples or *T. pseudonana* cultures, Figure S3C). If the difference between the two signals was more than one standard deviation above zero (see eq 1 in the Supporting Information), then it was flagged as being an observed product during the

https://doi.org/10.1021/acsearthspacechem.4c00163
ACS Earth Space Chem. 2024, 8, 1913−1923

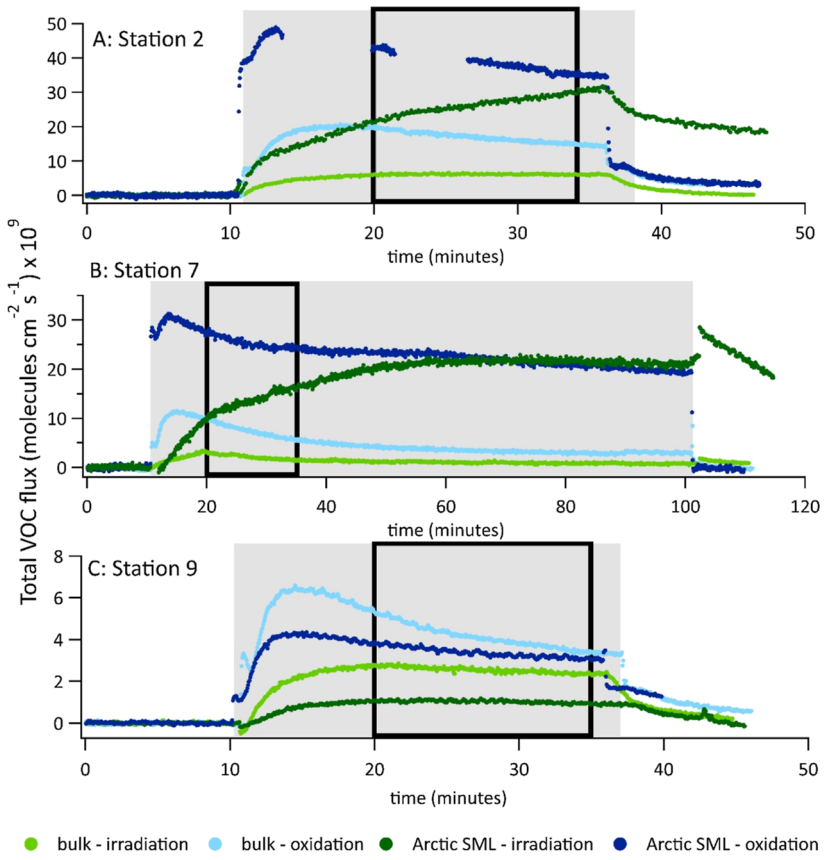

Figure 2. VOC emission profiles for each set of Arctic samples, for both irradiation and oxidation experiments. The vertical axis presents an estimate of the total VOC flux using the average sensitivity of the instrument. The three panels (A−C) represent the Arctic samples at stations 2, 7 and 9, respectively. The gray box represents the approximate time for which the samples were irradiated or oxidized. The start times for each experiment are identical within each plot, but the end times differ. The green traces represent the irradiation experiments, and the blue shades represent the oxidation experiments. The darker shades represent the Arctic SML sample, and the lighter shades represent the bulk water samples. The black box represents the time period used to calculate the average flux which is discussed in the following sections.

experiment. The ions produced during each Arctic seawater experiment are summarized in Table S3, and the ions produced during the *T. pseudonana* experiments are summarized in Table S4.

As the emission yield depended on time, and the temporal trend differed between oxidized and irradiated samples, averaged ion signals measured between 20 and 35 min after the start of the experiment (i.e., 10 to 25 min after the start of irradiation/oxidation) were chosen as the consistent time to compare the VOC yields between experiments.

RESULTS & DISCUSSION

Figure 2 presents the total VOC flux of identified ions from irradiation and oxidation of both the bulk and SML seawater samples. The periods highlighted in gray starting at 10 min represent the exposure of the samples to either light or ozone. The signals prior to 10 min have been zeroed and the background control has been subtracted, using the approach described above and in Figure S3.

The overall VOC yield was higher in the SML than the bulk samples for stations 2 and 7 (Figure 2A,B, respectively), but not for station 9 (Figure 2C). This trend held for both the irradiated and the oxidized samples. One possible explanation for this behavior is found in the surfactant and TOC measurements for each sample. At stations 2 and 7, surfactant and TOC concentrations were larger in the SML than in the bulk samples (although we note that the surfactant measurements were extremely variable; Table S1). At station 9, surfactant and TOC concentrations were higher in the bulk than in the SML samples. It is not uncommon for organic matter (including TOC and surfactants) to be depleted in the SML, and the degree of organic matter enrichment vs depletion in the SML is a result of variable environmental conditions and processes.[2,18] SML depletions are more often seen at lower windspeeds than under higher winds, which are thought to foster organic matter transport to the surface with bubble scavenging.[41,42] Without sufficient replenishment of organic matter in the SML, and with increased degradation or dilution processes (i.e., bacterial consumption, oxidation, rainfall), organic matter can be depleted in the SML.[43]

Parameterizing Total VOC Emissions. Oxidation experiments show an initial surge in VOC signal upon ozone exposure, which declines over time (Figure 2). When the ozone is switched off, the VOC signal rapidly drops. We hypothesize that the time-dependent VOC emissions are due to the consumption of reactive organics near the gas−liquid interface. Previous work, which used the same experimental setup to explore the reaction of gaseous ozone and aqueous iodide, showed the rapid consumption of iodide within the short reacto-diffusive depth of ozone, which is estimated to be approximately 2 μm with 390 nM iodide present in solution.[33] Similar behavior with the ozone-organic reaction is expected and has been observed in comparable flow tube experiments

https://doi.org/10.1021/acsearthspacechem.4c00163
ACS Earth Space Chem. 2024, 8, 1913−1923

oxidizing real seawater,[27] signifying that the reaction is likely sensitive to the replenishment of organic reactive precursors within the reacto-diffusive depth of ozone. It is also possible that the reaction occurs only at the gas−liquid interface, in which case, a supply of reactive precursors would also need to be maintained.

In contrast, the VOC signal from the irradiation experiments increases more slowly, to reach a steady-state production rate that is sustained over the length of the experiment. When the lights are turned off, the VOC signal is slower to return to baseline than in the oxidation experiments. For the irradiation experiments, the background production of VOCs from the empty glass tube is high with a similar temporal profile, making the interpretation of the results more challenging (Figure S4). Initially, the oxidation experiments produced more VOCs than the irradiation experiments, but over longer time periods (here, up to a maximum of 90 min, Figure 2B) the signals converged to reach similar, steady emission rates between the two mechanisms.

UV−visible light can penetrate meters into the ocean, deeper than the underlying seawater collected here at 0.2 m.[44,45] Release of VOCs that form deeper in the water column would depend on their aqueous lifetime and the rate of upward ocean mixing. A water-side transport limitation is supported by the emission profile of the total VOCs produced from irradiation, which suggested that the VOCs were formed throughout the solutions, leading them to be more slowly emitted over time relative to oxidation. Laboratory irradiation studies using surfactants to represent the SML (e.g., nonanoic acid) have demonstrated greater VOC emissions than from systems without surfactants, but those yields depended on the presence of photosensitizing material.[24,46−50]

The variability in total VOC yield from irradiation and oxidation processes presents a challenge in understanding the overall impact of these emissions on the marine atmosphere. To understand this variability, with a view to developing VOC emission parametrizations that could be used in numerical models (with caution, the caveats are discussed below in the Environmental Implications section), the total VOC yield was compared with seawater composition. Figure 3 illustrates the total VOC emissions from both irradiation and oxidation of the Arctic SML and bulk seawater samples as a function of the TOC and DOC concentrations, which we found to be the best available predictors of the total VOC emissions from these samples. This result is consistent with field measurements of atmospheric VOCs during the summer of 2014 in the same region where our samples were collected in 2016. Those 2014 measurements identified a marine source of oxygenated-VOCs measured via HR-ToF-CIMS with acetate as a reagent ion which correlated well with DOC concentrations of the bulk seawater collected at a depth of 2−5 m deep (r^2 = 0.82).[51] As DOC is usually the dominant component of TOC, it is likely that the VOC emission patterns are mostly driven by DOC. The linear correlation parameters for the relationships between total VOC emissions vs TOC and DOC, as well as chlorophyll *a*, heterotrophic bacteria, total phytoplankton (photosynthetic prokaryotes and eukaryotes), photosynthetic prokaryotes, TN, and TDN are presented in Table S5.

Parameterizing the Emissions of Individual Oxygenated VOCs. The dominant ion signal emitted from the SML samples for all oxidation and irradiation experiments (but for only one bulk sample, from station 9 in the oxidation experiment), was $[C_3H_7O]^+$ (Table S3). In PTR-MS spectra,

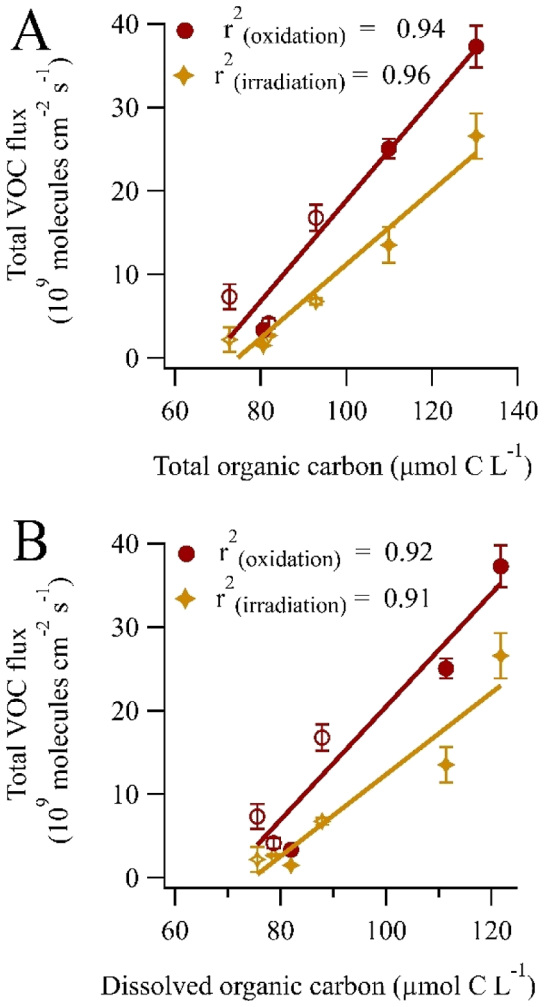

Figure 3. Total VOC flux from the Arctic SML and bulk water samples as functions of their (A) TOC and (B) DOC concentrations for both the irradiated (yellow stars) and oxidized (red circles) experiments. SML samples are marked with filled symbols, and bulk water samples are marked with empty symbols. The error bars represent the propagated 1σ uncertainty calculated from the difference of a 15 min measurement average of the experiment relative to background.

$[C_3H_7O]^+$ is usually attributed to acetone or propanal, which are structural isomers.[39] The acetone/propanal signal from irradiation is very well correlated with TOC (r^2 = 0.997, Figure 4A) and heterotrophic bacteria (r^2 = 0.999, Table S5). The emission of both acetone and propanal from the ocean is thought to be mostly due to photochemistry, and is well correlated with CDOM, which was not measured in our samples.[52,53] Previous measurements in the Arctic ocean have found CDOM absorbance is often linearly correlated with DOC.[51,54] Other observations of photochemical acetone emissions correlated well with cryptophyte and eukaryotic phytoplankton,[55] but we see no such correlation with phytoplankton abundances (r^2 = 0.22, Table S5).

Acetone/propanal emissions from the oxidation of ocean water are well parametrized by TOC (r^2 = 0.92, Figure 4A). The flux of acetone and propanal was previously measured in a similar setup using ocean water from the South China sea exposed to 100 ppbv of ozone.[26] The combined acetone and propanal fluxes from that study (on the order of 10^9 to 10^{10} molecules cm^{-2} s^{-1}) were comparable to our observations,

https://doi.org/10.1021/acsearthspacechem.4c00163
ACS Earth Space Chem. 2024, 8, 1913−1923

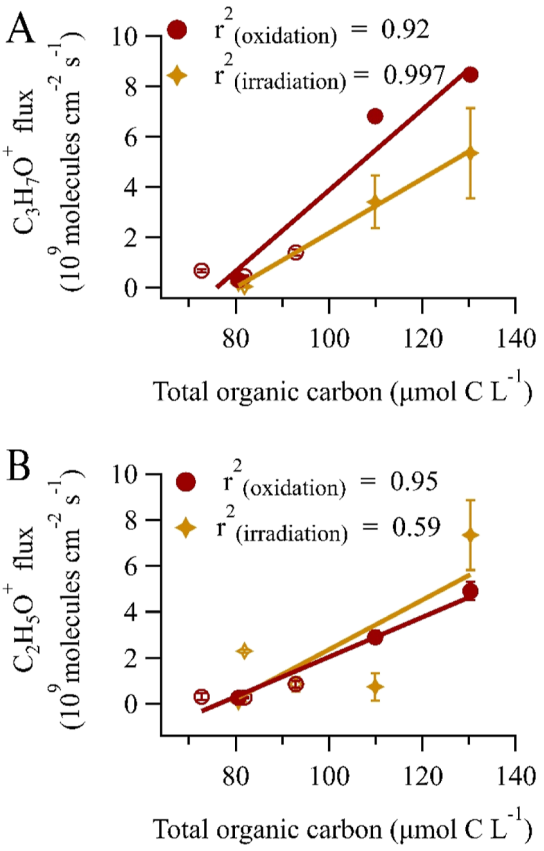

Figure 4. (A) Acetone/propanal (measured as $C_3H_7O^+$) flux and (B) acetaldehyde (measured as $C_2H_5O^+$) flux as functions of TOC for both the irradiated (yellow stars) and oxidized (red circles) experiments. SML samples are marked with filled symbols, and bulk water samples are marked with empty symbols. The error bars represent the propagated 1σ uncertainty calculated from the difference of a 15 min measurement average of the experiment relative to background. Note that in panel A, only four samples emitted the $C_3H_7O^+$ ion above the background when irradiated. In panel B, only five samples emitted the $C_2H_5O^+$ ion above the background when irradiated.

especially when considering the lower ozone mixing ratio of 45 ppbv used here. Previous measurements of acetone/propanal are observed during the oxidation of *T. pseudonana* cultures with ozone,[12] and from the oxidation of SML samples collected from the Canadian west coast and the eastern equatorial Pacific ocean.[17] On the other hand, neither propanal nor acetone emission was observed in oxidation experiments with ozone using seawater collected from Scripps Pier, in San Diego, California.[27]

The $[C_2H_5O]^+$ ion (commonly attributed to acetaldehyde) was the most abundant ion produced from the irradiation of the bulk water from station 9 (Table S3). We find that the emission of acetaldehyde can be roughly parametrized using the TOC content in the seawater (Figure 4B). For photosensitized chemistry, acetaldehyde emission can be well parametrized by the CDOM content of seawater, which was not measured in our samples.[16,53] Here, we found comparable emission rates of acetaldehyde from oxidation and irradiation. Previous work in our laboratory investigating indoor aldehyde emissions and behavior found that about 11% of the $C_2H_5O^+$ ion signal resulted from the fragmentation of larger ions, including $[C_3H_7O]^+$ (only propanal), $[C_5H_{11}O]^+$ (pentanal and 2-pentanone), $[C_6H_{13}O]^+$ (hexanal and 2-hexanone), $[C_7H_{15}O]^+$ (2-heptanone), and $[C_8H_{17}O]^+$ (octanal). All of these ions were observed in our oxidation experiments of Arctic ocean waters and are thus likely contributing to some degree to the $[C_2H_5O]^+$ signal we found in these samples. Kilgour et al. also noted a lack of acetaldehyde from the oxidation of the Scripps Pier seawater samples and used gas-chromatography which would separate the contribution of acetaldehyde to the $[C_2H_5O]^+$ ion from the fragmentation of larger ions.[27] Similar to this study, Wang et al. observed acetaldehyde with the PTR-ToF-MS from the oxidation of seawater from the South China sea, and positively identified it using an offline DNPH-derivation method.[26] Therefore, differences in observations are most likely related to the composition of the seawater.

Notably, there are high-intensity ions whose signals do not follow the same trends as the total VOC signal, i.e., TOC/DOC are not always the best predictors for the emissions of individual molecules. Consider the emission behavior of the $[C_9H_{19}O]^+$ ion, which is likely nonanal. This ion has been previously observed in SML oxidation experiments and has a relatively high m/z value compared to other observed ions, which reduces the likelihood that it results from the fragmentation of a heavier ion.[26,27] Additionally, the $[C_9H_{19}O]^+$ ion was the dominant ion emitted from the irradiation of station 2 bulk seawater (Table S3). Figure 5 illustrates the emission flux of nonanal as a function of TOC (Figure 5A) and phytoplankton abundance (Figure 5B). TOC is a poor predictor of nonanal emission for the oxidation experiments (r^2 = 0.09) but is the best predictor for the irradiation experiments (r^2 = 0.84), followed closely by heterotrophic bacteria (r^2 = 0.81). Conversely, phytoplankton abundance is the best predictor for nonanal emission from oxidation (r^2 = 0.72) but is a poor predictor of nonanal emission from irradiation (r^2 = 0.000002). Emission rates of nonanal from oxidation of seawater collected from the South China sea with 100 ppbv of ozone were slightly lower but similar to those observed from our experiments.[26]

Nonanal is the expected product arising from the reaction of ozone with a free- or triglyceride-containing 18:1ω9 fatty acid (i.e., oleic acid), which is commonly produced by *T. pseudonana* and oceanic phytoplankton species.[56] To confirm this, we oxidized *T. pseudonana* cultures to form the $C_9H_{19}O^+$ ion, which indicates that a phytoplankton exudate is a precursor to this ion (Figure S5). From this we infer that biological activity is an important driver of nonanal emission via oxidation of Arctic ocean waters. Conversely, we show that the *T. pseudonana* cultures result in very low nonanal emission during irradiation (Figure S5).

The dominant ion produced from oxidation of the bulk seawater samples from stations 2 and 7, was $[C_7H_{13}]^+$ (Table S3), which is commonly attributed to heptanal. Recent work found the $[C_7H_{13}]^+$ ion was also produced by the fragmentation of decanal ($[C_{10}H_{21}O]^+$) and $[C_{11}H_{23}O]^+$ ions,[27] both of which are found in all of our samples from both oxidation and irradiation experiments (Table S3) and could complicate our effort to parametrize heptanal emissions. $[C_7H_{13}]^+$ emission from oxidation is not well correlated with phytoplankton abundance (r^2 = 0.17) but is best correlated with chlorophyll α concentration (r^2 = 0.55), which suggests a photosynthetic connection. Similar to nonanal, $[C_7H_{13}]^+$ produced by irradiation is best described by TOC (r^2 = 0.95), but also has a better correlation with chlorophyll α

https://doi.org/10.1021/acsearthspacechem.4c00163
ACS Earth Space Chem. 2024, 8, 1913−1923

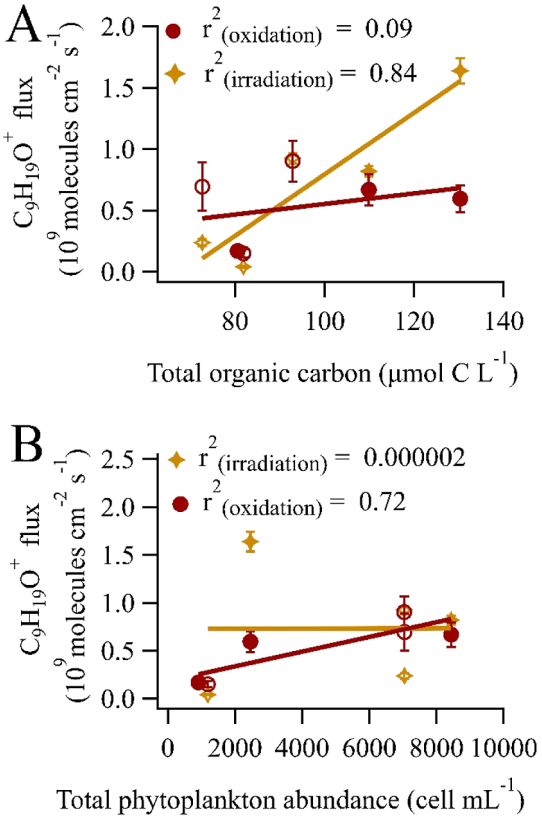

Figure 5. Estimated nonanal flux (measured as $C_9H_{19}O^+$) as functions of (A) TOC and (B) total phytoplankton abundance (including prokaryotes and eukaryotes (0.2−20 μm)) for both the irradiated (yellow stars) and oxidized (red circles) experiments. SML samples are marked with filled symbols, and bulk water samples are marked with empty symbols. The error bars represent the propagated 1σ uncertainty calculated from the difference of a 15 min measurement average of the experiment relative to background. Only five samples emitted the $C_9H_{19}O^+$ ion above the background when irradiated.

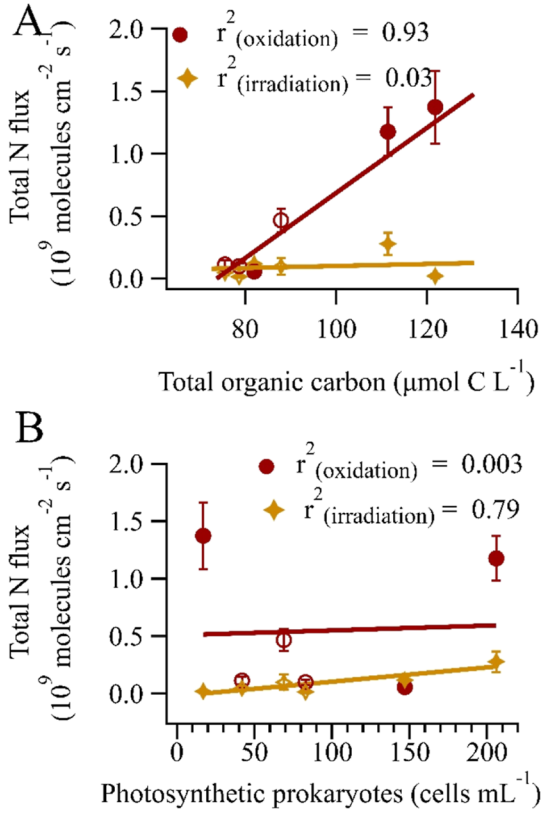

Figure 6. Estimated flux of the sum of all identified ions containing a N atom as functions of (A) TOC and (B) photosynthetic prokaryotes abundance for both the irradiated (yellow stars) and oxidized (red circles) experiments. SML samples are marked with filled symbols, and bulk water samples are marked with empty symbols. The error bars represent the propagated 1σ uncertainty calculated from the difference of a 15 min measurement average of the experiment relative to background.

concentration (r^2 = 0.57) than oxidation. During the oxidation of the *T. pseudonana* cultures, the $[C_7H_{13}]^+$ ion was readily produced (Figure S5), which likely arose from the oxidation of 16:1ω7 fatty acid as a free fatty acid or in its triglyceride form, which is abundantly produced by this culture.[56] The abundance of unsaturated fatty acids is known to be tied to the chlorophyll levels in Arctic waters.[57] Emission rates of heptanal from oxidation of seawater collected from the South China sea with 100 ppbv of ozone were an order of magnitude higher than what is reported in this study.[63] This could be due in part to the lower ozone mixing ratios used in our work, from the different water samples, or perhaps from different calibration procedures.

Parameterizing the Emission of Nitrogenated Compounds. In total, 14 nitrogenated ions were identified, as highlighted in yellow in Table S3. Figure 6A illustrates the sum of the identified nitrogenated ion fluxes as a function of TOC, which was a good predictor of nitrogenated VOC production from oxidation (r^2 = 0.93; Table S5), as is DOC (r^2 = 0.97, Table S5). TDN and TN were poor predictors (Table S5) of emitted nitrogenated VOCs from oxidation (r^2 = 0.12 and r^2 = 0.08, respectively), as were photosynthetic prokaryotes and total phytoplankton (photosynthetic prokaryotes and eukaryotes) abundances (r^2 = 0.003 and r^2 = 0.08, respectively).

In contrast, TOC was a poor predictor for nitrogenated VOC emission from irradiation (r^2 = 0.03), whereas photosynthetic prokaryotes abundance was the best (r^2 = 0.79). Photosynthetic prokaryotes, specifically cyanobacteria, are known for their ability to fix nitrogen and generate organic nitrogen.[58,5964] TDN and TN were fair predictors of nitrogenated VOC emission from irradiation (r^2 = 0.24 and r^2 = 0.18, respectively).

Recently, measurements of nitrogenated compounds have been observed from the oxidation of samples from the Chinese Pearl river and the SML in the South China sea.[26,28,60] In the gas phase, these compounds were identified by PTR-MS as being "azole-like", and were tentatively identified as $[C_4H_6NO]^+$ and $[C_5H_8NO]^+$ at unit mass resolution.[26] In our work, $[C_4H_6NO]^+$ was produced via oxidation of the station 2 SML sample, and both samples from station 9 (Table S3), but no $[C_5H_8NO]^+$ was observed above the background. However, the $[C_4H_6NO]^+$ ion was not the most abundant nitrogenated ion produced during oxidation in any of our samples; rather $[C_5H_{12}NO]^+$ dominated in the SML sample from station 2 and $[C_2H_6NO]^+$ in all the other samples. $[C_2H_6NO]^+$ was also the highest intensity nitrogenated ion for all irradiation experiments except again for the station 2 SML sample (which was dominated by $[C_5H_{12}NO]^+$) and the station 9 bulk water sample (dominated by $[C_4H_6NO_2]^+$). For the station 2 SML sample, the $[C_5H_{12}NO]^+$ ion likely arose

https://doi.org/10.1021/acsearthspacechem.4c00163
ACS Earth Space Chem. 2024, 8, 1913−1923

from acetamide, but fragmentation from a larger ion cannot be ruled out.

Overall, our results point to photosynthetic prokaryotes as important for the formation of nitrogenated VOCs from irradiation. To our knowledge, the emission of nitrogenated VOCs from the irradiation of seawater has not been previously observed. The precursors for nitrogenated VOCs from photosensitized chemistry and oxidation appear to originate from different sources, related more directly to photosynthetic prokaryote abundance versus the TOC pool, respectively.

Role of the SML. Lipids, carbohydrates, proteins, free amino acids, microgels and polysaccharides have all been measured in the SML in enriched concentrations and all have a biological origin.[7,18,61−63] The variability in enrichment factors for all these compounds is dependent on season, temperature, wind speed and location, making it difficult to generalize for the full ocean.[63] Enrichment of TOC and DOC has been sparsely measured in different regions, with factors ranging from 0.3 to 2.[64] The enrichment factors for the emissions of VOCs from our Arctic samples ranged from 0.04 to 25 (Figure S6), from strongly depleted to strongly enriched. There were also unique ions measured solely over the SML and not the bulk, which are highlighted in blue in Table S3. In total, irradiation produced 36, 45, and 4 characteristic SML ions (i.e., ions not observed in the bulk), and oxidation produced 19, 56, and 15 characteristic SML ions at stations 2, 7 and 9, respectively.

Enrichment factors that deviate from 1 emphasize the potential importance of Arctic SML composition on the yield of specific VOCs emitted to the atmosphere from irradiation and oxidation. Figures 3−6 illustrate how seawater composition can influence the emissions, highlighting the need to understand how the composition of the SML differs from the underlying water. The composition of the SML and particularly its variability remain uncertain, in part due to the uncertainty in formation and replenishment of species within the SML.

Environmental Implications. The results of the present study show that the oxidation and irradiation of Arctic SML and bulk waters lead to the emission of a similar suite of VOCs, which are dependent on water composition. The similar emission rates of total VOCs from oxidation and irradiation demonstrate that both mechanisms need to be evaluated to arrive at atmospherically relevant total VOC emission rates. The temporal profiles of VOC emissions are different for the two mechanisms (Figure 2), peaking early for oxidation, indicative of chemistry within a few microns of the interface, and later for photochemistry, which indicates chemistry occurring within the aqueous volume. The diminishing emissions rate in our oxidation experiments indicates that emission rates are likely controlled by the rate at which organic precursors are replenished in the actively exchanging surface volumes by both mass transfer and in situ production processes.

Beyond using field-collected Arctic seawater and SML samples, a novel aspect of this study is that we conducted both oxidation and irradiation experiments on the same samples, allowing us to determine the relative importance of the two emission mechanisms. Moreover, we examine correlations between VOC emissions and common measurements of oceanic composition. Among our findings, most prominent is that the intensity of the total VOC emissions correlates most tightly with organic matter concentrations in the samples. Importantly, this correlation is irrespective of whether the samples were from the SML or the bulk waters. Indeed, one of the three samples had higher TOC values in the bulk than in the SML, which led to higher emissions from the bulk sample than from the SML sample. This speaks to the need to understand the composition of not only the SML, but also the underlying bulk water. Whereas the bulk seawater feeds the Arctic SML, so that their compositions are linked to some degree, differences between the two may nevertheless play a role in the specific character of VOCs released (as illustrated in Figure S6).

The reacto-diffusive depth of ozone in the presence of ambient seawater concentrations of iodide is only a few microns,[33] substantially smaller than the estimated 80 μm thickness of the SML samples collected in this campaign. Thus, the material in our SML samples contained everything which would have been available for reaction with ozone in the natural environment. Currently, our ability to measure the composition of that narrower ozone reactive layer is still severely limited. Open questions also remain about the physical mixing and replenishment of species within the SML in relation to underlying water.

Phenomena such as secondary organic aerosol formation and the effects of VOCs on the oxidation capacity of the atmosphere in marine regions will be highly sensitive to the specific VOCs emitted, not only on the total VOC flux. To that end, this paper illustrates that the fluxes of specific molecules, such as nonanal and nitrogen-containing compounds, may depend on the specific character of the substrate. For example, the oxidation fluxes of the C9 and C7 aldehydes ($[C_9H_{19}O]^+$ and $[C_7H_{13}]^+$) are most strongly associated with the phytoplankton abundance and chlorophyll *a* concentration in the ocean, very likely because of the high associated unsaturated lipid content that can be oxidized with ozone. As a second example, the emission of nitrogenated VOCs via irradiation is best predicted by the photosynthetic prokaryote abundance of the seawater samples, which is likely from their role in nitrogen fixation.[52]

To verify the biological connections in this work, we used *T. pseudonana* as a model planktonic algae to elucidate how some precursors may be formed. Specifically, the *T. pseudonana* cultures produced both nonanal and heptanal (i.e., $[C_9H_{19}O]^+$ and $[C_7H_{13}]^+$) during oxidation, very likely via oxidation of biolipids produced by the phytoplankton. On the other hand, we observed no such fluxes during irradiation. This use of relatively well-understood model organisms complements the measurements made on the more complex Arctic seawater samples. The cultures were axenic (bacteria free), so they did not provide insight into the impacts of bacterial metabolism. Additionally, they are monocultures, which do not represent the full diversity of plankton producing lipids.

While there are very large uncertainties in extrapolating laboratory studies of a small number of collected samples from one specific environment to the global scale, a rough estimate can provide insight into the potential significance of the emission mechanisms studied in this work to global VOC budgets. In particular, by extrapolating the results of our six samples (i.e., both SML and bulk waters) to scale with the global area of the ocean, we can roughly estimate an annual VOC emission budget, assuming the number of carbon atoms in identified molecular formulas, or in the cases without an identified formula, by assuming a molecular structure with 5 carbons as was previously done by Novak and Bertram.[21] With

https://doi.org/10.1021/acsearthspacechem.4c00163
ACS Earth Space Chem. 2024, 8, 1913−1923

this approach, we calculate an emission range of 45−450 Tg C year^{-1} from oxidation, based on our lowest and highest yield experiments. This range of emissions is comparable to, but higher than, that of Novak and Bertram, who estimated emissions between 17.5 and 87.3 Tg C year^{-1}.[21] Measurements of VOC emission and ozone deposition rates from Scripps Pier resulted in annual estimate of VOC emission via oxidation between 12.6 and 136 Tg C year^{-1}.[27] In their discussion, Kilgour et al. suggested that laboratory experiments may overestimate VOC emission yields from heterogeneous ozonolysis, since laboratory experiments lack VOC loss pathways in the condensed phase, or because a stable microlayer may arise in the lab which is more enriched than in the environment.[27] Moreover, the small number of samples used in this study are spatially and temporally isolated to summer Arctic coastal waters, which may be more productive than the open ocean. These factors, combined with the relatively high mixing ratio of ozone (45 ppbv) we used in this study, relative to typical marine boundary layer ozone mixing ratios, suggest the range we measured is an upper-end estimate.

Using the same approach as above for oxidation, we calculate an annual emission by irradiation (assuming 50% of the day is irradiated) of 5−140 Tg C year^{-1}. This range is wider than, but similar to, an estimate of 23.2−91.9 Tg C year^{-1} derived from a global modeling study which parametrized VOC emissions using laboratory photochemical studies, wind speed, and global SML coverage.[65]

Scaling our acetaldehyde fluxes to the global ocean surface results in estimated emission rates between 0.4 and 30 Tg year^{-1} from irradiation and 2 to 40 Tg year^{-1} from oxidation. In comparison, a modeled total annual acetaldehyde oceanic emission rate of 19−31 Tg from the ocean, accounted for UV photolysis, but not oxidation.[66,67] Photosensitized production is thought to account for the majority (∼68%) of acetaldehyde emission into the atmosphere from the ocean.[52]

It is important to re-emphasize that the merit of these global flux extrapolations is simply to show the extent to which specific VOC emission mechanisms may be of significance to the gas phase organic carbon budget in the marine boundary layer; these values should be used in global models with extreme caution. More accurate assessments of total global VOC emission rates require field measurements at many locations and times across the globe. Our assessment is limited by the very small number of samples that were collected over a 3 week period in a small area of the eastern Canadian Arctic, which most certainly had a different oceanic organic composition and biological community than other times or other regions. Indeed, these kinds of measurements should be conducted in both oligotrophic and eutrophic regions. As well, our laboratory conditions do not fully match those in the environment with respect to ozone and light levels, and the issue of organic precursor replenishment can only be addressed in a field or, potentially, a mesocosm setting. However, the correlations we observed with specific measures of seawater composition, in particular for the total VOC fluxes and those of individual molecules, should be conceptually useful and may be generally applicable.

■ ASSOCIATED CONTENT

Data Availability Statement

The data used to generate the plots in this publication are available online (10.5683/SP3/MXAF7A).[68]

Supporting Information

The Supporting Information is available free of charge at https://pubs.acs.org/doi/10.1021/acsearthspacechem.4c00163.

Section 1 of the SI describes the Arctic sample collection and measurements, with the details in Table S1. Section 2 contains additional details on the experimental method. This includes experimental validation of our irradiation setup (Figure S2), calibration gases used for the PTR-MS (Table S2), and the data analysis workflow (Figure S3). Section 3 contains details on the experimental results. These include the master peak list for the Arctic experiments (Table S3) and the *T. pseudonana* culture experiments (Table S4), the time trace of the $[C_6H_{11}]^+$ ion in the experiment and blank (Figure S4), the production of the $[C_9H_{19}O]^+$ ion from *T. pseudonana* cultures (Figure S5), the r^2, slope and intercept between different VOCs and the Arctic water measurements (Table S5), and the enrichment factor of each ion for each SML/bulk sample pair (Figure S6) (PDF)

■ AUTHOR INFORMATION

Corresponding Author

Stephanie R. Schneider − *Department of Chemistry and Chemical Biology, McMaster University, Hamilton, Ontario M5S 3H6, Canada; Department of Chemistry, University of Toronto, Toronto, Ontario M5S 3H6, Canada;* orcid.org/0000-0002-6518-060X; Email: sschneid@ualberta.ca

Authors

Douglas B. Collins − *Department of Chemistry, Bucknell University, Lewisburg, Pennsylvania 17837, United States;* orcid.org/0000-0002-6248-9644

Matthew Boyer − *Institute for Atmospheric and Earth System Research (INAR)/Physics, Faculty of Science, University of Helsinki, Helsinki 00014, Finland*

Rachel Y.-W. Chang − *Department of Physics and Atmospheric Science, Dalhousie University, Halifax, Nova Scotia B3H 4R2, Canada*

Michel Gosselin − *Institut des sciences de la mer, Université du Québec à Rimouski, Rimouski, Québec G5L 3A1, Canada*

Victoria E. Irish − *Environmental Monitoring and Analysis Branch, BC Ministry of Environment and Climate Change Strategy, Smithers, British Columbia V0J 2N0, Canada*

Lisa A. Miller − *Institute of Ocean Sciences, Fisheries and Oceans Canada, Sidney, British Columbia V8L 4B2, Canada*

Jonathan P. D. Abbatt − *Department of Chemistry, University of Toronto, Toronto, Ontario M5S 3H6, Canada;* orcid.org/0000-0002-3372-334X

Complete contact information is available at: https://pubs.acs.org/10.1021/acsearthspacechem.4c00163

Notes

The authors declare no competing financial interest.

■ ACKNOWLEDGMENTS

We thank Jenna Ditto, Han Huynh, and Spiro Jorga for help with the PTR-MS measurements, Mélanie Simard for DOC and TDN analysis, Claude Belzile for flow cytometry analysis, Danielle Caleb for surfactant analyses, and Martine Lizotte,

Maurice Levasseur, Joannie Charette, Aude Boivin-Rioux and Marjolaine Blais for NETCARE oceanographic support, as well as Chief Scientists Christian Nozais and Tim Papakyriakou, Captain Alain Gariépy, and the crew of the CCGS Amundsen for enabling sample collection. We acknowledge NSERC and the Department of Fisheries and Ocean for graduate funding for S.R.S. and for operational support, including the NETCARE campaign.

REFERENCES

(1) Cunliffe, M.; Engel, A.; Frka, S.; Gašparović, B.; Guitart, C.; Murrell, J. C.; Salter, M.; Stolle, C.; Upstill-Goddard, R.; Wurl, O. Sea Surface Microlayers: A Unified Physicochemical and Biological Perspective of the Air-Ocean Interface. *Prog. Oceanogr.* **2013**, *109* (Supplement C), 104−116.

(2) Engel, A.; Bange, H. W.; Cunliffe, M.; Burrows, S. M.; Friedrichs, G.; Galgani, L.; Herrmann, H.; Hertkorn, N.; Johnson, M.; Liss, P. S.; Quinn, P. K.; Schartau, M.; Soloviev, A.; Stolle, C.; Upstill-Goddard, R. C.; van Pinxteren, M.; Zäncker, B. The Ocean's Vital Skin: Toward an Integrated Understanding of the Sea Surface Microlayer. *Front. Mar. Sci.* **2017**, *4*, 165.

(3) Coward, E. K.; Seech, K.; Carter, M. L.; Flick, R. E.; Grassian, V. H. Of Sea and Smoke: Evidence of Marine Dissolved Organic Matter Deposition from 2020 Western United States Wildfires. *Environ. Sci. Technol. Lett.* **2022**, *9* (10), 869−876.

(4) Guitart, C.; García-Flor, N.; Bayona, J. M.; Albaigés, J. Occurrence and Fate of Polycyclic Aromatic Hydrocarbons in the Coastal Surface Microlayer. *Mar. Pollut. Bull.* **2007**, *54* (2), 186−194.

(5) Song, Y. K.; Hong, S. H.; Jang, M.; Han, G. M.; Shim, W. J. Occurrence and Distribution of Microplastics in the Sea Surface Microlayer in Jinhae Bay, South Korea. *Arch. Environ. Contam. Toxicol.* **2015**, *69* (3), 279−287.

(6) Astrahan, P.; Herut, B.; Paytan, A.; Rahav, E. The Impact of Dry Atmospheric Deposition on the Sea-Surface Microlayer in the SE Mediterranean Sea: An Experimental Approach. *Front. Mar. Sci.* **2016**, *3*, 322.

(7) Cunliffe, M.; Upstill-Goddard, R. C.; Murrell, J. C. Microbiology of Aquatic Surface Microlayers. *FEMS Microbiol. Rev.* **2011**, *35* (2), 233−246.

(8) Liss, P. S.; Liss, P. S.; Duce, R. A. *The Sea Surface and Global Change*; Cambridge University Press: England, 2005.

(9) Cunliffe, M.; Wurl, O. *Guide to Best Practices to Study the Ocean's Surface*; Occasional Publications of the Marine Biological Association of the United Kingdom: Plymouth, UK, 2014.

(10) Rossignol, S.; Aregahegn, K. Z.; Tinel, L.; Fine, L.; Nozière, B.; George, C. Glyoxal Induced Atmospheric Photosensitized Chemistry Leading to Organic Aerosol Growth. *Environ. Sci. Technol.* **2014**, *48* (6), 3218−3227.

(11) Alpert, P. A.; Ciuraru, R.; Rossignol, S.; Passananti, M.; Tinel, L.; Perrier, S.; Dupart, Y.; Steimer, S. S.; Ammann, M.; Donaldson, D. J.; George, C. Fatty Acid Surfactant Photochemistry Results in New Particle Formation. *Sci. Rep.* **2017**, *7* (1), 12693.

(12) Schneider, S. R.; Collins, D. B.; Lim, C. Y.; Zhu, L.; Abbatt, J. P. D. Formation of Secondary Organic Aerosol from the Heterogeneous Oxidation by Ozone of a Phytoplankton Culture. *ACS Earth Space Chem.* **2019**, *3* (10), 2298−2306.

(13) Zhou, X.; Mopper, K. Photochemical Production of Low-Molecular-Weight Carbonyl Compounds in Seawater and Surface Microlayer and Their Air-Sea Exchange. *Mar. Chem.* **1997**, *56* (3−4), 201−213.

(14) Mopper, K.; Zhou, X.; Kieber, R. J.; Kieber, D. J.; Sikorski, R. J.; Jones, R. D. Photochemical Degradation of Dissolved Organic Carbon and Its Impact on the Oceanic Carbon Cycle. *Nature* **1991**, *353* (6339), 60−62.

(15) Kieber, D. J.; Mopper, K. Photochemical Formation of Glyoxylic and Pyruvic Acids in Seawater. *Mar. Chem.* **1987**, *21* (2), 135−149.

(16) Kieber, R. J.; Zhou, X.; Mopper, K. Formation of Carbonyl Compounds from UV-Induced Photodegradation of Humic Substances in Natural Waters: Fate of Riverine Carbon in the Sea. *Limnol. Oceanogr.* **1990**, *35* (7), 1503−1515.

(17) Zhou, S.; Gonzalez, L.; Leithead, A.; Finewax, Z.; Thalman, R.; Vlasenko, A.; Vagle, S.; Miller, L. A.; Li, S.-M.; Bureekul, S.; Furutani, H.; Uematsu, M.; Volkamer, R.; Abbatt, J. Formation of Gas-Phase Carbonyls from Heterogeneous Oxidation of Polyunsaturated Fatty Acids at the Air-Water Interface and of the Sea Surface Microlayer. *Atmos. Chem. Phys.* **2014**, *14* (3), 1371−1384.

(18) Wurl, O.; Ekau, W.; Landing, W. M.; Zappa, C. J. Sea Surface Microlayer in a Changing Ocean - A Perspective. *Elementa* **2017**, *5* (0), 31.

(19) Jenkinson, I. R.; Seuront, L.; Ding, H.; Elias, F. Biological Modification of Mechanical Properties of the Sea Surface Microlayer, Influencing Waves, Ripples, Foam and Air-Sea Fluxes. *Elementa* **2018**, *6* (1), 26.

(20) Frew, N. M. The Role of Organic Films in Air-Sea Gas Exchange. In *The Sea Surface and Global Change*; Cambridge University Press: England, 2009; pp 121−172.

(21) Novak, G. A.; Bertram, T. H. Reactive VOC Production from Photochemical and Heterogeneous Reactions Occurring at the Air-Ocean Interface. *Acc. Chem. Res.* **2020**, *53* (5), 1014−1023.

(22) Rossignol, S.; Tinel, L.; Bianco, A.; Passananti, M.; Brigante, M.; Donaldson, D. J.; George, C. Atmospheric Photochemistry at a Fatty Acid-Coated Air-Water Interface. *Science* **2016**, *353* (6300), 699−702.

(23) Fu, H.; Ciuraru, R.; Dupart, Y.; Passananti, M.; Tinel, L.; Rossignol, S.; Perrier, S.; Donaldson, D. J.; Chen, J.; George, C. Photosensitized Production of Atmospherically Reactive Organic Compounds at the Air/Aqueous Interface. *J. Am. Chem. Soc.* **2015**, *137* (26), 8348−8351.

(24) Trueblood, J. V.; Alves, M. R.; Power, D.; Santander, M. V.; Cochran, R. E.; Prather, K. A.; Grassian, V. H. Shedding Light on Photosensitized Reactions within Marine-Relevant Organic Thin Films. *ACS Earth Space Chem.* **2019**, *3* (8), 1614−1623.

(25) Saito, S.; Numadate, N.; Teraoka, H.; Enami, S.; Kobayashi, H.; Hama, T. Impurity Contribution to Ultraviolet Absorption of Saturated Fatty Acids. *Sci. Adv.* **2023**, *9* (38), No. eadj6438.

(26) Wang, Y.; Zeng, J.; Wu, B.; Song, W.; Hu, W.; Liu, J.; Yang, Y.; Yu, Z.; Wang, X.; Gligorovski, S. Production of Volatile Organic Compounds by Ozone Oxidation Chemistry at the South China Sea Surface Microlayer. *ACS Earth Space Chem.* **2023**, *7* (7), 1306−1313.

(27) Kilgour, D. B.; Novak, G. A.; Claflin, M. S.; Lerner, B. M.; Bertram, T. H. Production of Oxygenated Volatile Organic Compounds from the Ozonolysis of Coastal Seawater. *Atmos. Chem. Phys.* **2024**, *24* (6), 3729−3742.

(28) Wang, Y.; Deng, H.; Li, P.; Xu, J.; Jiang, B.; Pang, H.; Gligorovski, S. Molecular Characterization of the Product Compounds Formed upon Heterogeneous Chemistry of Ozone with Riverine Surface Microlayer. *J. Geophys. Res. Atmos.* **2022**, *127*, No. e2022JD037182.

(29) Chang, W.; Heikes, B. G.; Lee, M. Ozone Deposition to the Sea Surface: Chemical Enhancement and Wind Speed Dependence. *Atmos. Environ.* **2004**, *38* (7), 1053−1059.

(30) Sherwen, T.; Evans, M. J.; Carpenter, L. J.; Andrews, S. J.; Lidster, R. T.; Dix, B.; Koenig, T. K.; Sinreich, R.; Ortega, I.; Volkamer, R.; Saiz-Lopez, A.; Prados-Roman, C.; Mahajan, A. S.; Ordóñez, C. Iodine's Impact on Tropospheric Oxidants: A Global Model Study in GEOS-Chem. *Atmos. Chem. Phys.* **2016**, *16* (2), 1161−1186.

(31) Pound, R. J.; Sherwen, T.; Helmig, D.; Carpenter, L. J.; Evans, M. J. Influences of Oceanic Ozone Deposition on Tropospheric Photochemistry. *Atmos. Chem. Phys.* **2020**, *20* (7), 4227−4239.

(32) Luhar, A. K.; Woodhouse, M. T.; Galbally, I. E. A Revised Global Ozone Dry Deposition Estimate Based on a New Two-Layer Parameterisation for Air-Sea Exchange and the Multi-Year MACC Composition Reanalysis. *Atmos. Chem. Phys.* **2018**, *18* (6), 4329−4348.

(33) Schneider, S. R.; Lakey, P. S. J.; Shiraiwa, M.; Abbatt, J. P. D. Reactive Uptake of Ozone to Simulated Seawater: Evidence for Iodide Depletion. *J. Phys. Chem. A* **2020**, *124* (47), 9844−9853.
(34) Reeser, D. I.; Donaldson, D. J. Influence of Water Surface Properties on the Heterogeneous Reaction between O3(g) and I(Aq)-. *Atmos. Environ.* **2011**, *45* (34), 6116−6120.
(35) Mayer, K. J.; Sauer, J. S.; Dinasquet, J.; Prather, K. A. CAICE Studies: Insights from a Decade of Ocean-Atmosphere Experiments in the Laboratory. *Acc. Chem. Res.* **2020**, *53* (11), 2510−2520.
(36) Brüggemann, M.; Hayeck, N.; Bonnineau, C.; Pesce, S.; Alpert, P. A.; Perrier, S.; Zuth, C.; Hoffmann, T.; Chen, J.; George, C. Interfacial Photochemistry of Biogenic Surfactants: A Major Source of Abiotic Volatile Organic Compounds. *Faraday Discuss.* **2017**, *200*, 59−74.
(37) Schneider, S. R.; Lakey, P. S. J.; Shiraiwa, M.; Abbatt, J. P. D. Iodine Emission from the Reactive Uptake of Ozone to Simulated Seawater. *Environ. Sci.: Processes Impacts* **2023**, *25*, 254−263.
(38) Irish, V. E.; Hanna, S. J.; Xi, Y.; Boyer, M.; Polishchuk, E.; Ahmed, M.; Chen, J.; Abbatt, J. P. D.; Gosselin, M.; Chang, R.; Miller, L. A.; Bertram, A. K. Revisiting Properties and Concentrations of Ice-Nucleating Particles in the Sea Surface Microlayer and Bulk Seawater in the Canadian Arctic during Summer. *Atmos. Chem. Phys.* **2019**, *19* (11), 7775−7787.
(39) Pagonis, D.; Sekimoto, K.; de Gouw, J. A Library of Proton-Transfer Reactions of H3O+ Ions Used for Trace Gas Detection. *J. Am. Soc. Mass Spectrom.* **2019**, *30* (7), 1330−1335.
(40) Kind, T.; Fiehn, O. Seven Golden Rules for Heuristic Filtering of Molecular Formulas Obtained by Accurate Mass Spectrometry. *BMC Bioinf.* **2007**, *8* (1), 105.
(41) Kuznetsova, M.; Lee, C.; Aller, J.; Frew, N. Enrichment of Amino Acids in the Sea Surface Microlayer at Coastal and Open Ocean Sites in the North Atlantic Ocean. *Limnol. Oceanogr.* **2004**, *49* (5), 1605−1619.
(42) Wurl, O.; Wurl, E.; Miller, L.; Johnson, K.; Vagle, S. Formation and Global Distribution of Sea-Surface Microlayers. *Biogeosciences* **2011**, *8* (1), 121−135.
(43) Mustaffa, N. I. H.; Badewien, T. H.; Ribas-Ribas, M.; Wurl, O. High-Resolution Observations on Enrichment Processes in the Sea-Surface Microlayer. *Sci. Rep.* **2018**, *8* (1), 13122.
(44) Lee, Z.; Hu, C.; Shang, S.; Du, K.; Lewis, M.; Arnone, R.; Brewin, R. Penetration of UV-visible Solar Radiation in the Global Oceans: Insights from Ocean Color Remote Sensing. *J. Geophys. Res., C: Oceans Atmos.* **2013**, *118* (9), 4241−4255.
(45) Tedetti, M.; Sempéré, R. Penetration of Ultraviolet Radiation in the Marine Environment. A Review. *Photochem. Photobiol.* **2006**, *82* (2), 389−397.
(46) Ciuraru, R.; Fine, L.; Pinxteren, M. v.; D'Anna, B.; Herrmann, H.; George, C. Unravelling New Processes at Interfaces: Photochemical Isoprene Production at the Sea Surface. *Environ. Sci. Technol.* **2015**, *49* (22), 13199−13205.
(47) Ciuraru, R.; Fine, L.; van Pinxteren, M.; D'Anna, B.; Herrmann, H.; George, C. Photosensitized Production of Functionalized and Unsaturated Organic Compounds at the Air-Sea Interface. *Sci. Rep.* **2015**, *5*, 12741.
(48) Stirchak, L. T.; Abis, L.; Kalalian, C.; George, C.; Donaldson, D. J. Differences in Photosensitized Release of VOCs from Illuminated Seawater versus Freshwater Surfaces. *ACS Earth Space Chem.* **2021**, *5* (9), 2233−2242.
(49) Chiu, R.; Tinel, L.; Gonzalez, L.; Ciuraru, R.; Bernard, F.; George, C.; Volkamer, R. UV Photochemistry of Carboxylic Acids at the Air-Sea Boundary: A Relevant Source of Glyoxal and Other Oxygenated VOC in the Marine Atmosphere. *Geophys. Res. Lett.* **2017**, *44* (2), 1079−1087.
(50) Bernard, F.; Ciuraru, R.; Boréave, A.; George, C. Photosensitized Formation of Secondary Organic Aerosols above the Air/Water Interface. *Environ. Sci. Technol.* **2016**, *50* (16), 8678−8686.
(51) Mungall, E. L.; Abbatt, J. P. D.; Wentzell, J. J. B.; Lee, A. K. Y.; Thomas, J. L.; Blais, M.; Gosselin, M.; Miller, L. A.; Papakyriakou, T.; Willis, M. D.; Liggio, J. Microlayer Source of Oxygenated Volatile Organic Compounds in the Summertime Marine Arctic Boundary Layer. *Proc. Natl. Acad. Sci. U.S.A.* **2017**, *114* (24), 6203−6208.
(52) Dixon, J. L.; Beale, R.; Nightingale, P. D. Production of Methanol, Acetaldehyde, and Acetone in the Atlantic Ocean. *Geophys. Res. Lett.* **2013**, *40* (17), 4700−4705.
(53) Zhou, X.; Mopper, K. Photochemical Production of Low-Molecular-Weight Carbonyl Compounds in Seawater and Surface Microlayer and Their Air-Sea Exchange. *Mar. Chem.* **1997**, *56* (3−4), 201−213.
(54) Évrard, A.; Fink-Mercier, C.; Galindo, V.; Neumeier, U.; Gosselin, M.; Xie, H. Regulated vs. Unregulated Rivers: Impacts on CDOM Dynamics in the Eastern James Bay. *Mar. Chem.* **2023**, *256*, 104309.
(55) Lawson, S. J.; Law, C. S.; Harvey, M. J.; Bell, T. G.; Walker, C. F.; de Bruyn, W. J.; Saltzman, E. S. Methanethiol, Dimethyl Sulfide and Acetone over Biologically Productive Waters in the Southwest Pacific Ocean. *Atmos. Chem. Phys.* **2020**, *20* (5), 3061−3078.
(56) Zhukova, N. Changes in the Lipid Composition of Thalassiosira Pseudonana during Its Life Cycle. *Russ. J. Plant Physiol.* **2004**, *51*, 702−707.
(57) Marmillot, V.; Parrish, C. C.; Tremblay, J.-É.; Gosselin, M.; MacKinnon, J. F. Environmental and Biological Determinants of Algal Lipids in Western Arctic and Subarctic Seas. *Front. Environ. Sci.* **2020**, *8*, 538635.
(58) Flores, E.; Herrero, A. Nitrogen Assimilation and Nitrogen Control in Cyanobacteria. *Biochem. Soc. Trans.* **2005**, *33* (1), 164−167.
(59) Zehr, J. P. Nitrogen Fixation by Marine Cyanobacteria. *Trends Microbiol.* **2011**, *19* (4), 162−173.
(60) Wang, Y.; Deng, H.; Li, P.; Xu, J.; Loisel, G.; Pang, H.; Xu, X.; Li, X.; Gligorovski, S. Interfacial Ozone Oxidation Chemistry at a Riverine Surface Microlayer as a Source of Nitrogen Organic Compounds. *Environ. Sci. Technol. Lett.* **2022**, *9* (6), 493−500.
(61) Cunliffe, M.; Murrell, J. C. The Sea-Surface Microlayer Is a Gelatinous Biofilm. *ISME J.* **2009**, *3* (9), 1001−1003.
(62) Carpenter, L. J.; Nightingale, P. D. Chemistry and Release of Gases from the Surface Ocean. *Chem. Rev.* **2015**, *115* (10), 4015−4034.
(63) Carlson, D. J. Dissolved Organic Materials in Surface Microlayers: Temporal and Spatial Variability and Relation to Sea State. *Limnol. Oceanogr.* **1983**, *28* (3), 415−431.
(64) Engel, A.; Galgani, L. The Organic Sea-Surface Microlayer in the Upwelling Region off the Coast of Peru and Potential Implications for Air-Sea Exchange Processes. *Biogeosciences* **2016**, *13* (4), 989−1007.
(65) Brüggemann, M.; Hayeck, N.; George, C. Author Correction: Interfacial Photochemistry at the Ocean Surface Is a Global Source of Organic Vapors and Aerosols. *Nat. Commun.* **2018**, *9* (1), 3222.
(66) Millet, D. B.; Guenther, A.; Siegel, D. A.; Nelson, N. B.; Singh, H. B.; de Gouw, J. A.; Warneke, C.; Williams, J.; Eerdekens, G.; Sinha, V.; Karl, T.; Flocke, F.; Apel, E.; Riemer, D. D.; Palmer, P. I.; Barkley, M. Global Atmospheric Budget of Acetaldehyde: 3-D Model Analysis and Constraints from in-Situ and Satellite Observations. *Atmos. Chem. Phys.* **2010**, *10* (7), 3405−3425.
(67) Wang, S.; Hornbrook, R. S.; Hills, A.; Emmons, L. K.; Tilmes, S.; Lamarque, J.; Jimenez, J. L.; Campuzano-Jost, P.; Nault, B. A.; Crounse, J. D.; Wennberg, P. O.; Kim, M.; Allen, H.; Ryerson, T. B.; Thompson, C. R.; Peischl, J.; Moore, F.; Nance, D.; Hall, B.; Elkins, J.; Tanner, D.; Huey, L. G.; Hall, S. R.; Ullmann, K.; Orlando, J. J.; Tyndall, G. S.; Flocke, F. M.; Ray, E.; Hanisco, T. F.; Wolfe, G. M.; St Clair, J.; Commane, R.; Daube, B.; Barletta, B.; Blake, D. R.; Weinzierl, B.; Dollner, M.; Conley, A.; Vitt, F.; Wofsy, S. C.; et al. Atmospheric Acetaldehyde: Importance of Air-Sea Exchange and a Missing Source in the Remote Troposphere. *Geophys. Res. Lett.* **2019**, *46* (10), 5601−5613.
(68) Schneider, S. *Data for "Abiotic Emission of Volatile Organic Compounds from the Ocean Surface: Relationship to Seawater Composition*, 2024.

https://doi.org/10.1021/acsearthspacechem.4c00163
ACS Earth Space Chem. 2024, 8, 1913−1923